CHAPTER VI

INTRUSIVES

6.1 Introduction

There are two intrusive rocks in the study area. They are amphibolite (epidiorite) and granite. The amphibolite is well exposed at five stations of the investigated area (Map -1). In the field, the presence of the rock is characterized by yellowish brown soil cover, greenish coloured rock and the typical spheroidal weathering which is well observed on the boulder of this rock at Mawryngkneng (Photo-6.1a). The trend of the rock is parallel to that of the quartzite. So they are considered as sills in the Shillong Group of rocks.

The granite rock is often encountered at Kshehpongdeng and Shormo in the investigated area (Map-1). The rocks are massive and compact and the boulders show spheroidal weathering (Photo-6.1b). From the trend of the exposure the rock is considered as sills in the country rocks.

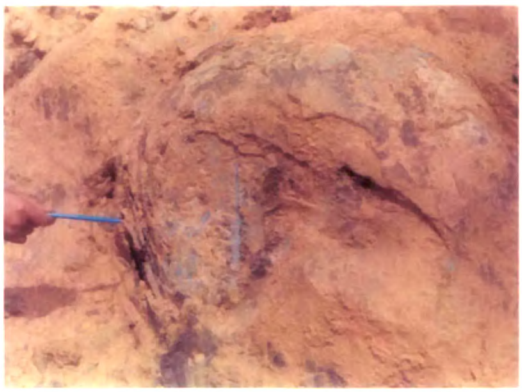

Photo 6.1a Amphibolite showing spheroidal weathering. (Locality- Mawryngkneng)

Photo 6.1b An exposure of granite. (Locality- Keshpongdeng)

6.2 Amphibolite

The dominant intrusive rock exposed in the study area is amphibolite. It is a metabasic rock with dominant mineral amphibole imparted a green colour to the rock, for which Oldham (1858) named it "Greenstone", but at a later date Medlicott (1869) called it "Khasi Greenstone" because of its occurrence in the Khasi Hills.

6.2.1 Megascopic characters

The amphibolite is characteristically coarse to medium grained rocks. It is dark green in colour and unweathered amphibolite shows prominent green colour but weathered variety shows reddish colour. It is hard and compact having moderately high specific gravity. It is massive and not foliated. In the coarse grained granular amphibolites, coarse cumulates of mafic minerals predominantly (Photo-6.1c). Such cumulates average 1cm. in size and appear to be made up of prismatic crystals with a rectangular or square outline. The cleavages are sometimes discernable and are vitreous in luster. The grains making up the groundmass are fine in size and subordinate in amount as compared to the cumulates. The medium grained amphibolites are generally granular and sometimes crudely foliated. They have a spotty appearance (Photo-6.1d), where blue-black grains of pyroxene are surrounded by a groundmass of few bluish green colourd epidote with minor light coloured fine laths of plagioclase.

Photo 6.1c Cumulate structure in amphibolite (Locality-Mawryngkneng)

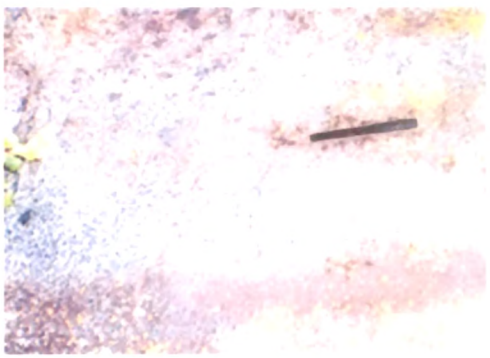

Photo 6.1d Weathered cumulates showing spotty appearance. (Locality- Nongpoh)

6.2.2 Microscopic characters

The amphibolites are composed of amphibole, plagioclase, with minor amount of quartz, pyroxene, epidote, biotite, iron oxides and sphene. Minerals such as apatite, chlorite and sericite (the latter two of secondary origin) also occur as accessories.

Amphibole: It is observed that amphibole occurs in three forms, viz ; as large idioblasts, as slender prisms and as needles. Large idioblasts are the most abundant form and are followed by slender prisms and needles. It has also observed that idioblasts of amphibole occur as large plates and as large 6-sided idioblastic crystals (Photo-6.2a). At the same time well formed amphiboles are also observed with zagged ends (Photo-6.2b). They are multicoloured and are pleochroic from light green to bluish green with nearly straight extinction in prismatic section. The other large amphibole plates show pleochroism from pale yellow green to dark green with extinction angle upto 15^0, which are identified as hornblende. The sieve structures within the idioblastic plates show common inclusions of plagioclase, iron oxides,magnetite, quartz and sphene (Photo-6.2c). Some of these idioblast show secondary alteration to actinolite and epidote, sometimes found in a core of the original hornblende; while some other amphiboles retain the typical pyroxene cleavage thus indicating their alteration from pyroxene.

It has observed that the slender prisms and needles of amphibole show pleochroic from light green to dark green, and sometimes to bluish green. The prismatic cleavage is also distinct. Such grains are often found to criss-cross one another and exhibit decussate texture. Pleochroic scheme of idioblastic hornblende shows strong pleochroism X = yellowish green, Y = light green, Z = bluish green X<Y<Z ; $Z\Lambda C = 10^0$-18^0. The sodic amphibole showing strong pleochroism X = light green Y = dark green Z = bluish green X<Y<Z; $Z\Lambda C = 0^0$. The amphibole needles show pleochroism X= yellowish green, Y= brownish, Z = bluish green X<Y<Z; $Z\Lambda C = 2^0$-5^0.

The amphibole are of at least two different generations. It has observed that inclusions of iron oxides, plagioclase, quartz and a few sphene with sieve structure and the coarser amphiboles contain inclusions of smaller needle-shaped grains of the same mineral.

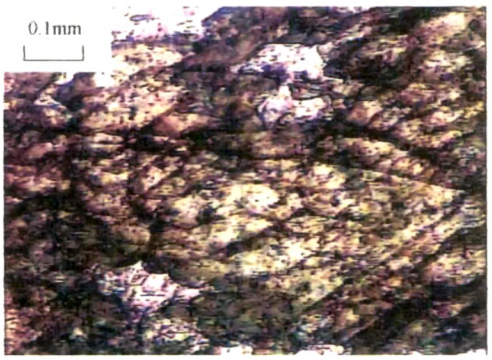

Photo 6.2a Well developed hornblende crystal occurs as large plate in amphibolite. Under polarized x10. (Locality- Nongplist)

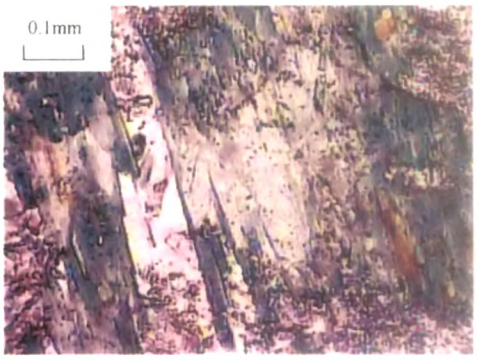

Photo 6.2b Well formed amphibole with zagged ends in amphibolite. Under polarized x10 (Locality- Mawryngkneng)

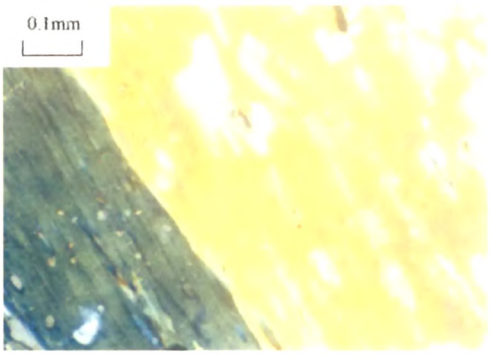

Photo 6.2c Sieve structure of hornblende in amphibolite. Crossed polarized x10 (Locality- Nongplist)

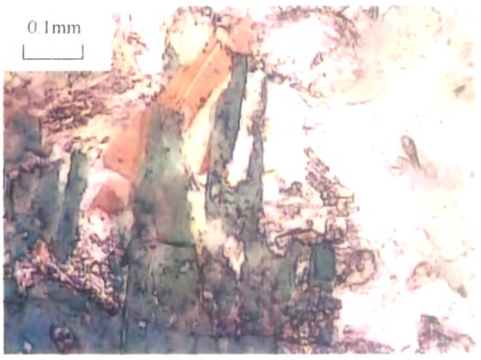

Photo 6.2d Biotite showing secondary growth in amphibolite. Under polarized x10 (Locality-Shormo)

Plagioclase : Plagioclase is the only feldspar mineral in the rock. They occur as fine to medium grained lath-shaped subhedral crystals with low relief and refractive index. The grains are colouriess with grey interference colour. The grains show polysynthetic twinning. The angle of extinction measured on albite twin varies from 10^0 to 12^0. The plagioclase mainly oligoclase in composition.

Quartz : Quartz occurs as anhedral grains of variable sizes and shapes. It also occurs as inclusions in hornblende and plagioclase. The grains are with low relief and low refractive index. It is colourless with grey interference colour. A few grains show weavy extinction.

Pyroxene (augite): Augite occurs as prismatic grains with high relief and high refractive index. The prismatic section shows one set of cleavage and the basal section are with two sets of cleavage which are at right angles. Mineral in most cases completely altered with a relict cave of the mineral in hornblende. Slender prisms of plagioclase are sometimes found as inclusion within large plates of pyroxene.

Biotite : Biotite occurs as fine prisms and needles. They are pale yellow in colour and pleochroic X = Yellow, Y = greenish yellow, Z = deep brown. Extinction is parallel and show high order of interference colour. It occurs as secondary origin (Photo-6.2d).

Sphene : Sphene is present in small crystals as well as irregular shaped grains. The colour observed is light yellowish brown. It is difficult to see the extinction positions because of the high degree of interference colours.

Magnetite : Magnetite is opaque . It occurs as angular grains, showing metallic lusture under reflected light. Magnetite makes the skeletal structure or relicts of pyroxene cleavage and can be traceable at the core of hornblende (Fig-6.1, Photo-6.3a).

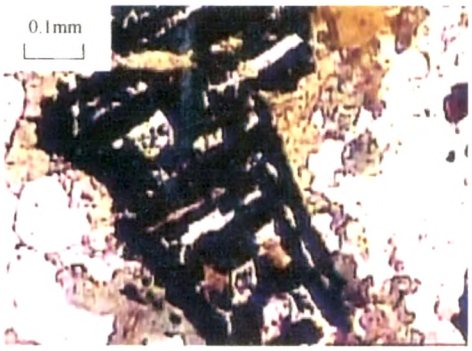

Photo 6.3a . Magnetite makes the skeletal structure of pyroxene cleavage in amphibolite. Crossed polarized x10. (Locality- Ksehpongdeng)

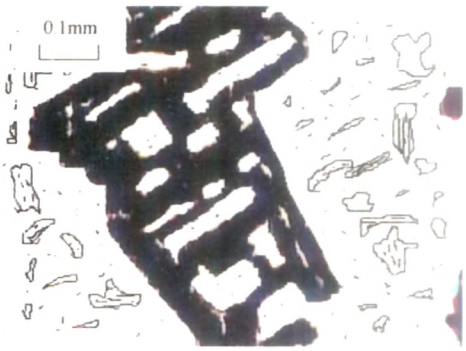

Fig.6.1 Magnetite in amphibolite retaining skeletal structure of pyroxene. Locality- Ksehpongdeng.

Epidote : Epidote occurs as elongated and granular crystals. The grains are green in colour and feebly pleochroic. It exhibits anomalous interference colours of green, yellow, pink, red etc. Extinction is parallel when measured in elongated sections. Epidote has probably been resulted from the alteration of calcic plagioclase or hornblende because grains are intimately associated with plagioclase and hornblende.

6.2.3 Texture

Coarse grained amphibole occurs as porphroblasts with irregular margins. Such porphyroblasts occur as large plates (Photo-6.2a). They also exhibit sieve structure with inclusion of plagioclase, sphene and iron oxides (Fig-6.2, Photo-6.2c). Magnetite shows typical skeletal structure of pyroxene cleavage (Photo-6.3a). The porphyroblasts are uniformly distributed over the whole rock. The amphibole and pyroxene porphyroblasts are set in a groundmass of fine to medium grained subidioblastic plagioclase and quartz besides needles of amphibole and biotite. The texture exhibited is distinctly porphyroblastic (Photo-6.3b).

The prisms and laths of amphibole sometimes exhibit penetration twins (Photo-6.3c).Traces of ophitic texture is often observed due to the development of plagioclase laths inside the hornblende crystals (Fig-6.3, Photo-6.3d). Schistosity is shown by sub-parallel to parallel arrangement of hornblende grains.

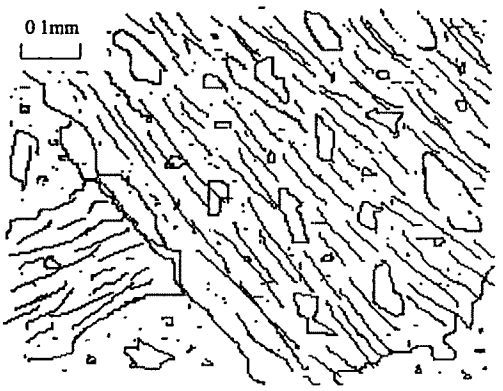

Fig.6.2 Hornblende plate showing sieve structure in amphibolite. Locality- Nongplit

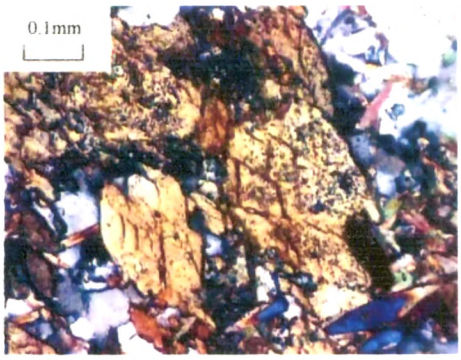

Photo 6.3b Hornblende porphyroblast in groundmass of plagioclase quartz and biotite in amphibolite. Crossed polarized x10 (Locality- Mawryngkneng)

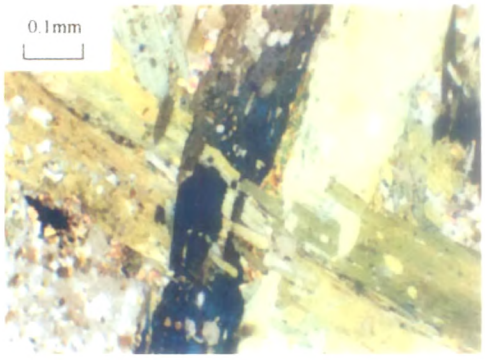

Photo 6.3c Penetration twin showing by hornblende in amphibolite. Crossed polarized x10 (Locality- Ksehpondeng

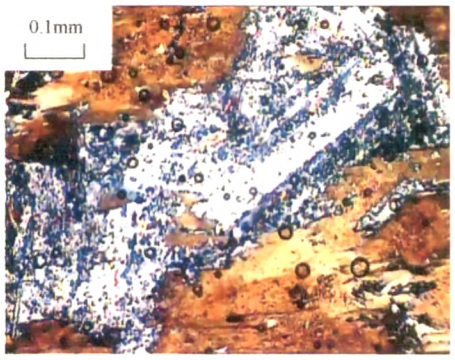

Photo 6.3d Large hornblende plate in amphibolite poikilitically enclosing plagioclase, exhibiting ophitic texture. crossed polarized x10 (Locality-Shormo)

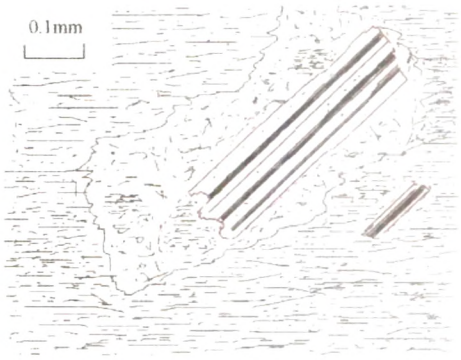

Fig.6.3 Plagioclase laths inside the hornblende showing ophitic texture in amphibolite. Locality- Shormo.

6.2.4 Modal Analysis

The modal analysis of four samples of amphibolites taken from different localities of the area are determined and shown in the table 6.1. From the modal composition it is clear that amphibole and plagioclase together forms more then 90% of the rock.

The percentage of hornblende along with the remnants of pyroxene varies from 62.20% to 74.85%. The plagioclase value ranges, between 21.07% to 25.23%. The quartz percentage is vary low, between 2.15% to 7.07%. The percentage of the rest of the minerals ranges from 1.86% to 6.71%.

Table 6.1 Model composition of amphibolite of the area vol.%

	Ksehpongdeng	Shormo	Mawryngkneng	Nongplit
Amphibole	62.20	65.54	71.94	74.95
Plagioclase	25.23	23.27	22.36	21 07
Quartz	5.86	7.07	3.84	2 15
Others	6.71	4.12	1.86	1.93
Total	100.00	100.00	100.00	100.00

6.2.5 Petrochemistry of amphibolite

Amphibolites occurring in five different localities and five samples have been chemically analyzed for major oxides and have been shown in table-6.2 along with CIPW norm and Niggli values.

The composition of amphibolites is more or less uniform in all five areas The Al_2O_3 varies from 11.96% to 15.55%, TiO_2 from 0.39% to 0.82%, iron oxides from 7.73% to 10.33%, MgO from 3.91% to 6.12%, CaO from 6.50% to 9.49%, MnO from 0.02% to 0.34% and Na_2O from 0.39% to 0.74%.

In the ACF ternary diagram (after, Fyfe *et al.*, 1954) plot of the rock are within the basic igneous rock. All the plots are indicative of magmatic origin as the amphibolites lie within the field of igneous rocks and also within the closed contours of both Miyashiro (1973), M, and Heier (1962), H (Fig-6.4).

Plots of MgO against CaO of the amphibolite are seen to follow differentiation trend of continental tholeiite (CT) from Skeargard as shown in figure-6.5 (after Wager and Mitchel, 1951 taken from Floyed, 1976). All the plots in SiO_2

against Na_2O + K_2O diagram (Fig-6.6) fall in the tholeiitic field It is observed that, due to low alumina content these plots are in tholeiitic field In the (FeO^t+TiO_2) – Al_2O_3 – MgO triangular diagram (after Jensen, 1976) the amphibolite are seen to be iron tholeiites as the plots in the HFT field (Fig-6.7).

From the Niggli mg against c diagram (after Leake, 1964) it is observed that rocks fall in the middle to late stage differentiates (Fig-6.8). In the Niggli si versus mg plot (Fig-6.9), all the samples show the distinct igneous trend besides plotting in the field of igneous rocks. The igneous trend is also shown in the 100mg – c – (al-alk) diagram of Leake (1964) where the amphibolites follow the trend of the Karoo Dolerites (Fig-6.10).

The Niggli values (al-alk) versus c (Van de Kamp, 1968) all the samples fall within the igneous field (Fig-6.11). The amphibolites are seen as ortho-amphibolites from the mg versus alk, mg versus k and mg versus ti diagram where all the samples plot in the ortho fields (Fig-6.12). This is more or less in consonance when the samples are plotted in Niggli (al-alk) versus c plot, where all the samples lie within the igneous field (Evans and Leake, 1960) and approximately within the field of the Karoo Dolerites (fig-6.13).

Finally an attempt has been made to find the tectonic setting of the amphibolites. So the TiO_2 – 10MnO – P_2O_5+1 tectonic plot of Mullen (1983) is used (Fig-6.14). It is observed that all the samples fall in the island arc tholeiitic field. Again the TiO_2 – K_2O - P_2O_5 (Pearce *et al.*, 1975) and FeO^t – MgO – Al_2O_3 (Pearce *et al.*, 1977) triangular diagrams show that the amphibolites are non-oceanic basalts which seem to have been intruded near the continental margin (Fig-6.15 and Fig-6.16).

Table 6.2 : Major element composition for the amphibolite of the area (wt%)

Major Oxides	SP-01	SP-02	SP-03	SP-04	SP-05
SiO_2	63.75	63.85	62.74	58.23	58.37
TiO_2	0.39	0.49	0.57	0.72	0.82
Al_2O_3	12.82	11.96	15.55	14.09	13.39
Fe_2O_3	1.00	1.10	2.39	1.55	2.21
FeO	7.23	7.33	5.34	8.02	8.12
MnO	0.08	0.18	0.02	0.24	0.34
MgO	3.91	4.01	4.68	5.92	6.12
CaO	9.39	9.49	6.50	9.10	9.20
Na_2O	0.39	0.49	0.57	0.64	0.74
K_2O	0.91	0.87	1.62	1.30	0.40
P_2O_5	0.13	0.23	0.02	0.19	0.29

CIPW Norm

Quartz	30.60	30.48	29.28	19.02	21.72
Orthoclase	5.00	5.00	9.45	7.22	2.22
Albite	3.14	4.19	4.71	5.24	6.28
Anorthite	30.58	27.80	31.90	31.97	31.97
Wallastonite	6.26	7.30	1.02	5.10	4.98
Diopside	5.67	4.75	11.60	14.80	15.30
Hypersthene	15.90	17.02	6.86	12.27	11.61
Magnetite	1.39	1.39	3.48	2.08	3.24
Illmenite	0.60	0.91	1.06	1.36	1.52
Apatite	0.33	0.67	0.03	0.33	0.67

Niggli Values

al	24.75	23.12	31.27	23.67	22.62
fm	39.20	40.11	39.09	44.59	46.28
c	33.06	33.39	24.27	27.78	28.32
alk	2.79	3.35	5.34	3.94	2.76
si	210.09	209.88	214.81	166.20	167.70
k	0.33	0.37	0.31	0.30	0.69
mg	0.40	0.41	0.33	0.31	0.30
qz	98.21	96.48	93.45	50.44	56.66
p	0.19	0.19	0.03	0.17	0.34
ti	0.79	1.18	1.44	1.54	1.72

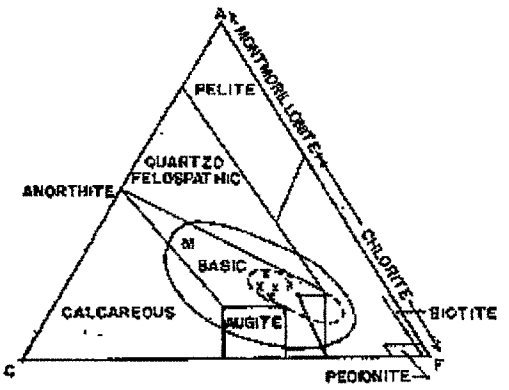

Fig.6.4 $A(Al_2O_3+Fe_2O_3-Na_2O-K_2O)$- $C(CaO-3.3P_2O_5)$- F(FeO+MgO+MnO) plots of amphibolite (after Fyfe *et al.*,1958). Superimposed area the field at basic rocks after Miyashiro(1973), M, and Heier (1962), H.

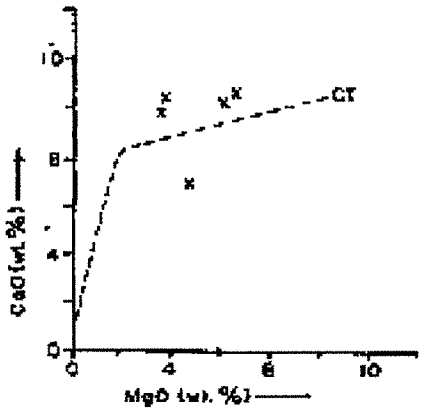

Fig.6.5 Plots of MgO against CaO of the analyzed amphibolite. The differentiation trend for continental thoeleiite (CT) from Skaergaard (after Wager and Mitchell, 1951, taken from Floyd, 1976) is given for comparison.

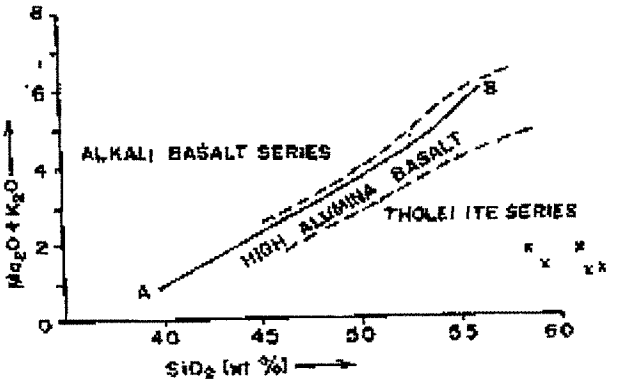

Fig.6.6 SiO_2 versus (Na_2O+K_2O) diagram for the analyzed amphibolites. Line AB divides the field of alkali basalts and tholeiitic basalts (after McDonald and Kastura, 1964) over which Kuno's (1966) field of high alumina basalt is suterimposed.

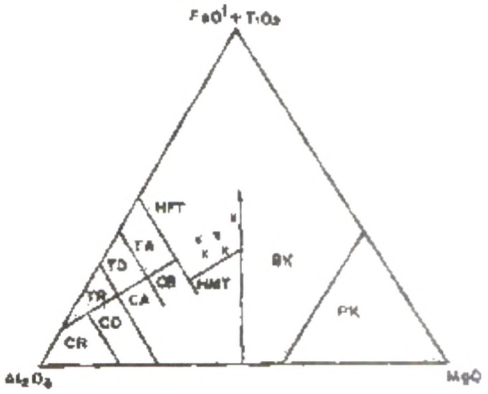

Fig.6.7 Al_2O_3-(FeO+TiO_2)-MgO triangular diagram (after Jensen, 1976) for the amphibolite. HFT-high iron tholeiitic ; HMT-high magnesian tholeiitic ; CB-calc basalt ; TA- tholeiitic andesite; CA- calc andesite; TD- tholeiitic dacite; CD- calc dacite; TR- tholeiitic rhyolite; CR-calc rhyolite; BK- basalt komatiite; PK- picrite komatiite.

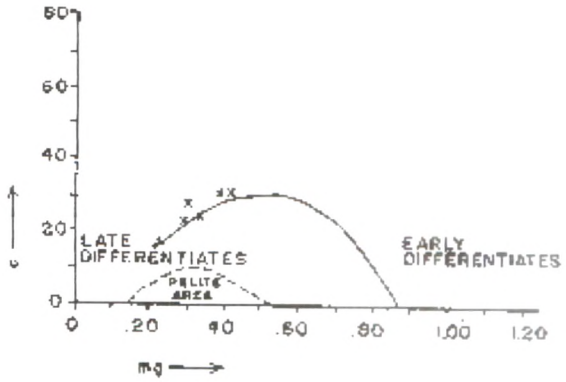

Fig.6.8 Plots of Niggli **mg** against **c** (after Leake, 1964) for the analyzed amphibolite. The area inside the continuous and dotted line represent the field of igneous and pelitic rocks respectively.

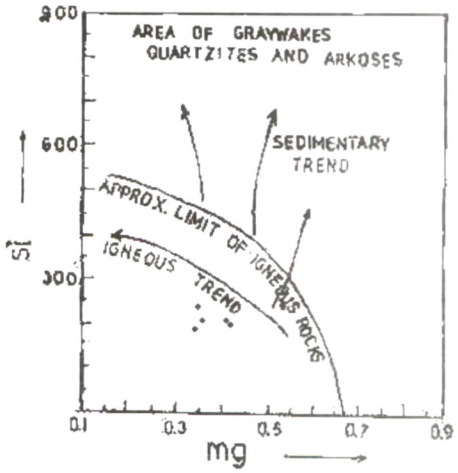

Fig.6.9 Niggli **mg** versus **si** plots of the analysed amphibolites.

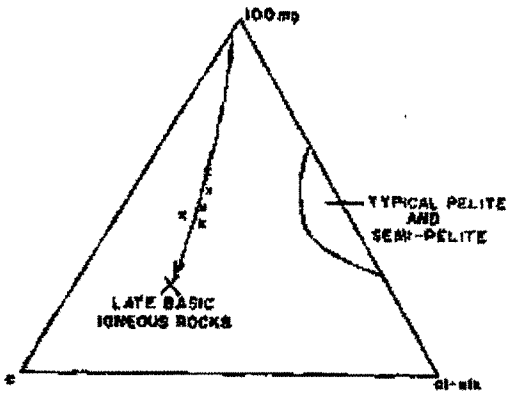

Fig.6.10 c - 100mg - (al-alk) triangular plots (after Leake, 1964) of the analyzed amphibolites.

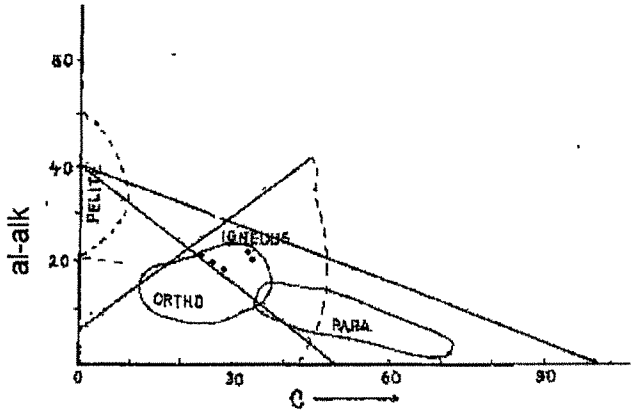

Fig.6.11 Plots of Niggli **c** against (al-alk) after Van de Kemp, 1968, of the analyzed amphibolites.

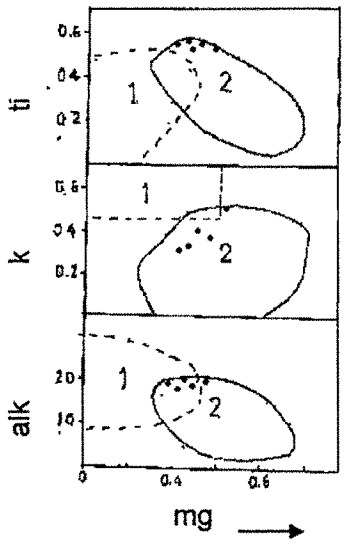

Fig.6.12 Plots of Niggli **mg** against **alk, k** and **ti** of the analyzed amphibolites.
1- pelitic rocks; 2- ortho- amphibolite.

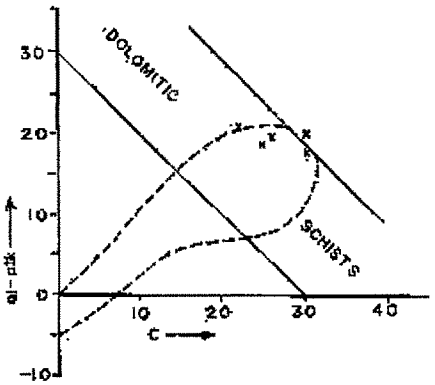

Fig.6.13 Plots of Niggli **c** against (al-alk) (after Leake, 1964) for the analyzed amphibolites. The broken line indicating the composition of the Karroo dolerite (after Evans and Leake, 1960) is given for comparison.

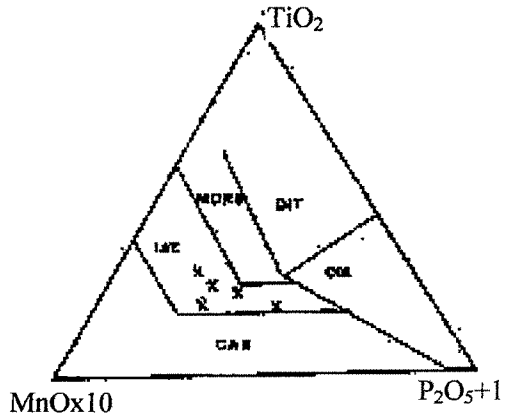

Fig.6.14 MnOx10 – TiO_2 – P_2O_5+1 tectonic plots (after Mullen, 1983) of the analyzed amphibolites. OIT- ocean island tholeiitic; MORB- mid-oceanic ridge basalt; IAT- island arc tholeiitic; CAB- calc alkaline basalt; OIA- ocean island andesite.

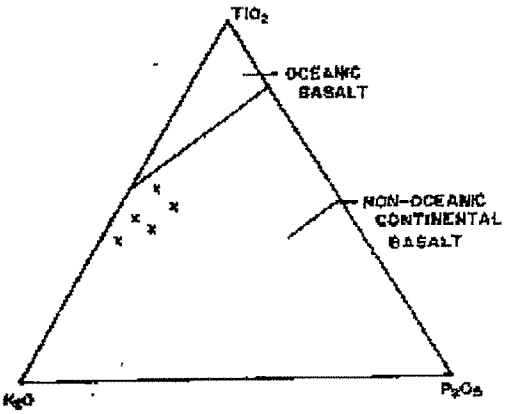

Fig.6.15 K_2O- SiO_2 – P_2O_5 triangular plots (after Pearce *et al.*, 1975) for the analyzed amphibolites.

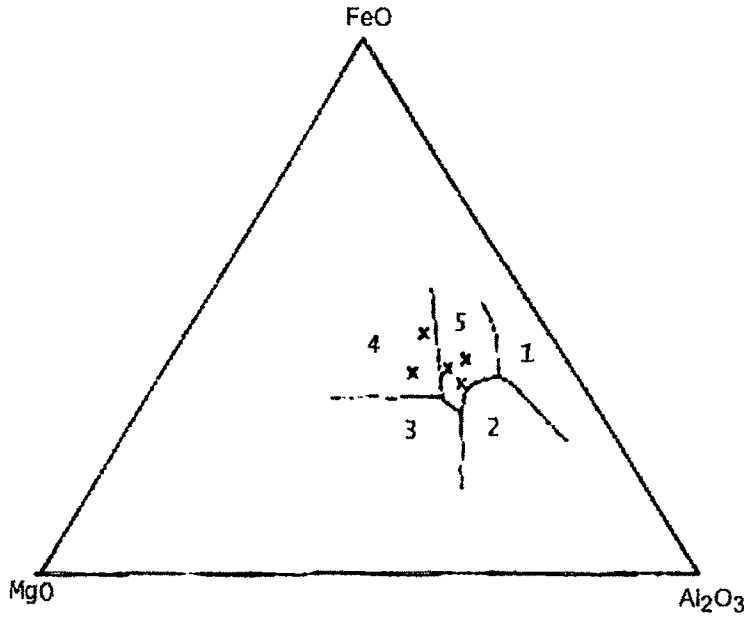

Fig.6.16 MgO- FeO – Al_2O_3 tectonic plots (after Pearce *et al.*, 1977) for the analyzed amphibolites. 1- spreading centre island; 2- orogenic ; 3- ocean ridge and floor; 4- ocean island; 5- continental.

6.2.6 Metamorphism

The amphibolite intruded into the rocks of the Shillong Group. A derivative of basic igneous rock and suffered regional metamorphism simultaneously with the host (Shillong Group). Due to this the original ferromagnesian minerals, augite and plagioclase are subjected to alteration, the pyroxene is converted to amphibole and calcic plagioclase breaking down to a secondary sodic plagioclase, thus exhibiting retrogressive effects.

The original augite is almost altered to amphibole due to uralitisation. Quartz which is present in small quantities as interstitial grains in the groundmass, is derived as a byproduct in the process of uralitisation of the pyroxene to amphibole. Magnetite shows some interesting characteristics. It is present as skeletal structures often pseudomorphous after clino-pyroxene grain with pyroxene cleavage (Photo-6.3a). Magnetites present in the groundmass are accessory minerals of the original basic rock and those forming skeletal structures are all of secondary derivation when original pyroxenes are converted to amphibole.

Along with uralitisation the process of saussuritisation has also operated whereby the calcic plagioclase is altered to secondary sodic plagioclase. The plagioclases which have altered to a mass of fine grained albite, clinoziosite, epidote, sericite and quartz retain their original tabular crystal shapes. The few grains of biotite formed after hornblende also signifies the retrogressive metamorphism attained by the rock (Photo-6.2d).

6.2.7 Origin of the amphibolite

Amphibolites are intrusive into the quartzite and metapelite of the Shillong Group of rocks as concordant or discordant body. From the field occurrence, mineral characters, texture, structure and geochemistry, it is clear that the

amphibolite is basic igneous rock of tholeiitic nature. Evidences in support of this view are listed below:

1. It occurs as sills (in the study area) and also as dyke in the quartzite and metapelite of the Shillong Group.
2. The nature of the contacts between the amphibolite and the host rocks is sharp.
3. It is massive and non-foliated.
4. It is hard and compact with high specific gravity.
5. Textures and structures like skeletal structures of pyroxene, amphibolite pseudomorphous after relict pyroxene, unaltered pyroxene cores and interpenetration twins in amphiboles indicate their basic igneous rock parentage.
6. Formation of hornblende has resulted mainly from clinopyroxene through the process of Uralitisation.
7. Magnetites of secondary derivation from the metamorphic process from skeletal structures pseudomorphing original pyroxene (Photo-6.3a).
8. The petrochemical study of the amphibolites support that the amphibolites were derived from a basic igneous rock of tholeiitic composition. The various petrochemical diagrams supporting igneous parentage are stated below:

a. The amphibolite plots show an igneous trend (Fig-6.10) and fall in the ortho- amphibolite field (Fig-6.11, Fig-6.12).
b. The amphibolites are early to middle stage differentiates (Fig-6.8).
c. The amphibolites show a tholeiitic trend (Fig-6.6).
d. A closed affinity to Karroo Dolerites is noticed (Fig-6.13).
e. Tectonic plots indicate that the amphibolites are continental or non-oceanic basalts intruded near continental margins (Fig-6.14, Fig-6.15 and Fig-6.16).

6.3 Granite

There are two granite bodies in the study area (Map-1). One is at Ksehpongdeng (Field spot) and another is at Shormo (Field spot) They are intrusive body within the quartzite of the Shillong Group. It is massive and nonfoliated. The general alignment of the granite body is E-W to NE-SW, conformable with the tectonic axis or the major lineaments (ENE-WSW) of the Shillong Plateau. The granite bodies of various dimentions occur as plutons in the Khasi Hills, of which Myllieum, Umroi and Weiloi plutons are noteworthy.

6.3.1 Megascopic characters

The Granite is light grey, coarse grained, rich in k-feldspar (microcline) which occurs as intrusive body. It is a massive body with more hardness. . Quartz is identified by its vitreous lusture. The main character of the granite body is that it contains hypersthene. So it may be named as 'Hypersthene granite'.

6.3.2 Microscopic characters

Granite is composed of quartz, microcline, pyroxene (hypersthene), plagioclase, muscovite, biotite,zircon, apatite, epidote etc.

Potash-feldspar: - It constitutes the major portion of the rock. It occurs as large platy, tabular, subhedral to anhedral grains. The grains are characterized by perthitic structure (Fig-6.17, Photo-6.4a). Microcline occurs as coarse to medium grained subhedral to anhedral grains. It is colourless and show grey to variable interference colour due to alteration and crossed hatched twinning (Photo-6.4b).

Fig.6.17 Perthitic intergrowth of potash feldspar and plagioclase in granite. Locality:- Ksehpongdeng.

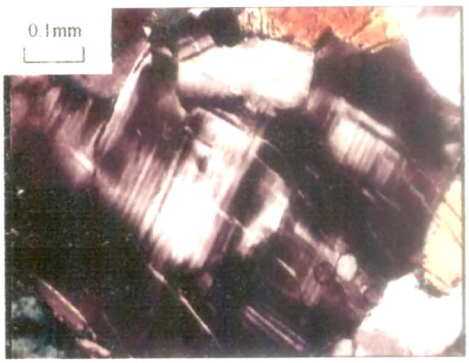

Photo-6.4a: Perthite in potash feldspar. Cross polars x 10 (Locality- Ksehpongdeng)

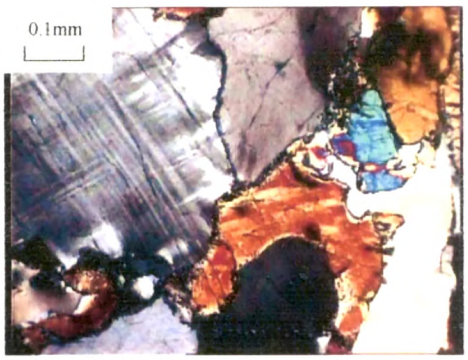

Photo-6.4b: Cross-hatched twinning shown by microcline in granite. Cross polars x 10 (Locality- Ksehpongdeng)

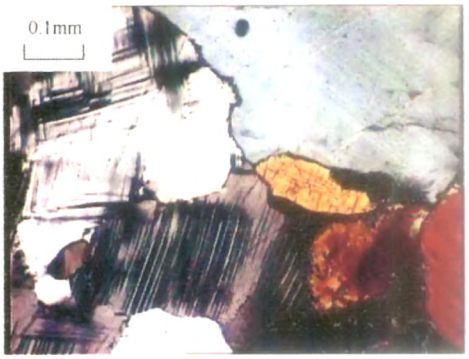

Photo-6.4c: Plagioclase showing perthitic intergrowith microcline in granite. Cross polars x 10 (Locality- Ksehpongdeng)

Quartz: - Grains are mostly coarse in size. All grains are characterized by low relief and refractive index, colourless with grey interference colour and weavy to straight extinction. It contains inclusion of needles of rutile.

Plagioclase: - It occurs as lath-shaped subhedral crystals with low relief and refractive index. Plagioclase is found in the form of (i) parthite occurring within microcline (Photo-6.4c) and (ii) oligoclase developing as individual grains. Grains are colourless with grey interference colour. Polysynthetic twinning is well developed (Photo-6.4d). The angle of extinction on albite twinning varies from 0^0 to 12^0.

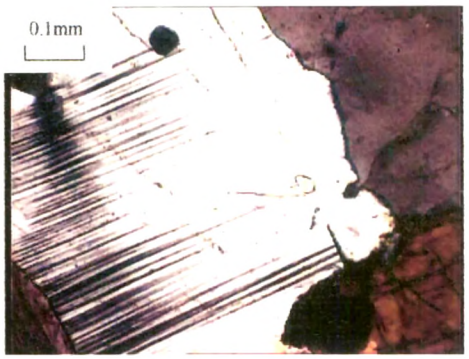

Photo-6.4d: Plagioclase showing polsynthetic twinning in granite. Cross polars x 10 (Locality- Ksehpongdeng)

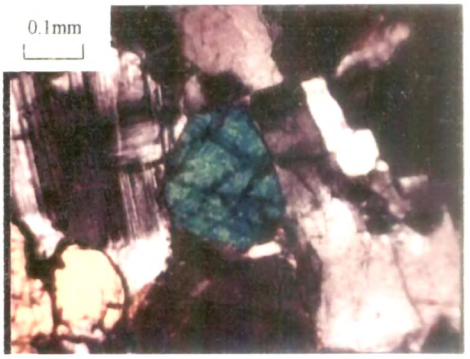

Photo-6.5a: Hypersthene showing well developed cleavage in granite. Cross polars x 10 (Locality- Ksehpongdeng)

Hypersthene: - It is coarse to medium grained and show high order interference colours. Prismatic crystals have well developed pyroxene cleavage (Photo-6.5a). The rhombic-pyroxene has distinct pleochroism from pink to green, X = pink, Y = yellow, Z = green. The grains have high refractive index and parallel extinction.

Augite: - It occur as subhedral prismatic grains with high relief and refractive index. Coarse prismatic grains show one set of distinct cleavage. They are pale green to slight green and slightly pleochroic. Extinction measured on prismatic grains vary from 38° to 45°.

Biotite: - It occurs as tabular subhedral grains with high relief and refractive index. The grains show one set of distinct cleavage. It is strongly pleochroic from brownish yellow to light yellow. Extinction is straight and show high order interference colour. Biotites are altered to epidote and chlorite.

Epidote: - It occurs as elongated and granular crystals. The grains show yellowish green colour and feebly pleochroic. It exhibits anomalous interference colours (green, yellow, pink etc.). Extinction is parallel when measured in elongated section.

Chlorite: - It is flaky in habit with high relief and refractive index. It is green in colour and strongly pleochroic. The minerals show high order interference colour. The extinction is straight.

Magnetite: - The magnetite occurs as irregular grain. It is black in colour and shows matellic lusture under transmitted light. Smaller grains of minerals are in association with epidote and chlorite.

Zircon: - It is anhedral and also characteristics overgrowth and intergrowth. It is colourless and extinction is straight (Photo-6.5b).

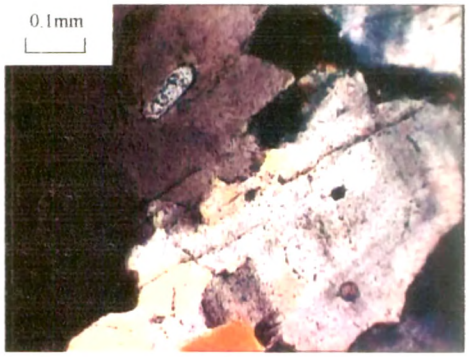

Photo-6.5b: Euhedral zircon in granite. Cross polars x 10 (Locality- Kschpongdeng)

Apatite: - It is present as inclusions as well as interstitial grain. Grains are mostly needle shaped. They are colourless with grey interference colour and show straight extinction.

6.3.3 Texture

Under microscope the rock is even-grained and is composed of quartz and potash-feldspar with oligoclase, ortho-pyroxene and iron oxides and occasional crystal of zircon. Hence the texture of this rock is hypidiomorphic granular (Fig-6.18, Photo-6.5c). The quartz is blue, grey or greenish and usually is filled with innumerable acicular crystals and having parallel extinction. The potash-feldspar is usually microcline and frequently microcline-

microperthite. The microcline together with quartz forms the greater part of the rock. The plagioclase in the rock itself is oligoclase. The rhombic-pyroxene has distinct pleochroism, pink to green and parallel extinction. Myrmekitic intergrowth of quartz and plagioclase feldspar in which the quartz occurs as worm-like rods within the feldspar (Fig-6.19, Photo-6.5d). It is generally the result of the replacement of potash feldspar by soda-rich plagioclase feldspar with separation of excess quartz.

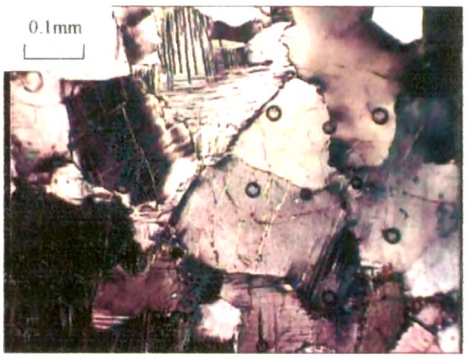

Photo-6.5c Granite showing hypidiomorphic granular texture. Cross polars x 10 (Locality- Ksehpongdeng)

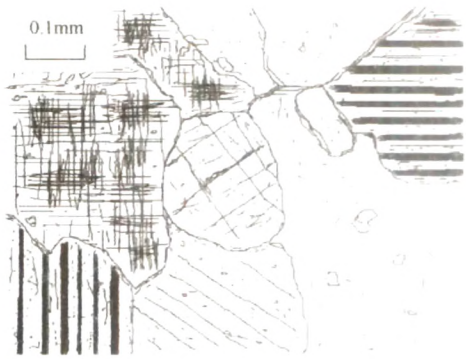

Fig.6.18 Hypidiomorphic granular texture in granite. Locality:- Ksehpongdeng.

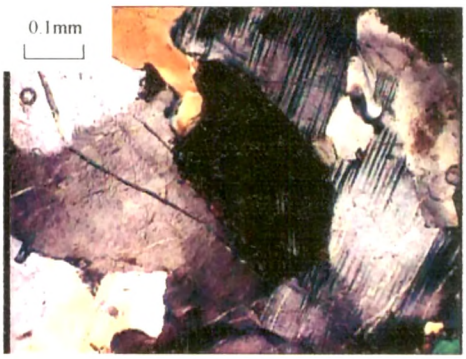

Photo-6.5d Myrmekitic intergrowth of quartz and plagioclase in granite. Cross polars x 10(Locality- Ksehpongdeng)

Fig.6.19 Mymekitic intergrowth of quartz and plagioclase in granite. Locality- Ksehpongdeng

6.3.4 Modal Analysis

The modal analysis of four samples of granites taken from different localities of the area are determined and shown in the table 6.3. The percentage of k-feldsper varies from 19.36% to 28.53%. The plagioclase value varies from 34.06% to 39.82%. The quartz percentage varies from 18.45% to 22.26%. Hypersthene and augite together varies from 13.92% to 16.00%. The percentage of the rest of the minerals ranges from 2.15% to 3.36%.

Table 6.3 Model composition of granite of the area vol.%

	SN-1	SN-2	SN-3	SN-4
K-feldspar	28.10	19.36	28.53	25.08
Plagioclase	38.37	39.82	34.06	39.28
Quartz	20.68	22.26	20.33	18.45
Hypersthene	10.26	08.47	09.25	07.65
Augite	04.23	07.53	05.58	06.27
Others	03.36	02.56	02.15	03.27
Total	100.00	100.00	100.00	100.00

6.3.5 Petrochemistry of the Granite

Three samples are analysed for their major oxides in order to determine the petrochemical characteristics of the granite (Table 6.4). The SiO_2 ranges from 58.92% to 64.24%, Al_2O_3 from 13.57% to 16.32%, Fe_2O_3 from 0.97 to 4.01, FeO from 4.88% to 7.10%, MnO from 0.12 to 0.24, MgO from 1.36% to 4.09%, CaO from 5.16% to 6.83%, Na_2O from 3.65% to 4.00%, K_2O from 0.42% to 1.27%, P_2O_5 from 0.17% to 0.26% and TiO_2 from 0.84% to 1.51 percent.

In the ACF triangular diagram after Chappell & White (1992) the granites are metaluminous in composition (Fig-6.20). In metaluminous materials, the mole percentage alumina is less than the combined mole percentage of lime, soda and potash, but greater than the combined mole percentage of soda and potash ($CaO + Na_2O + K_2O > Al_2O_3 > Na_2O + K_2O$).

In the QAP diagram the plots of all samples fall in the granite field (Fig-6.21).The An – Ab – Or triangular diagram of O'Connor (1965) shows that the granite plots are in the tonalite field (Fig-6.22). Similarly in the Al_2O_3 - K_2O - CaO triangle diagram of Ali and Rao (1980), also the sample plots are in the tonalite field (Fig-6.23). The normative Or—Ab—An triangular diagram with compositional field after Iden(1981) and the binary Al_2O_3—K_2O diagram after Harpam (1963) also show the sample plots in the tonalite field (Fig-6.24 & Fig-6.25).

According to the diagram SiO_2 versus Na_2O+K_2O of Irvine and Baragar (1971) granites are identified as subalkaline type (Fig 6.26).

The study also emphasis to determine the source material of the granite. In the Na_2O/Al_2O_3 versus K_2O/Al_2O_3 plot (after Garrels & Mckenzie, 1971), the source material may be igneous rocks (Fig-6.27). In other plots Na_2O versus K_2O (after Cheppel and White 1992, Fig-6.28) and Na_2O versus K_2O (after Hine *et al.* 1978, Fig-6.29) the samples plot is closer to the I-type granite field.

In the SiO_2 versus FeO/FeO+MgO variation diagram (Fig-6.30) and SiO_2 vs. Al_2O_3 (Fig-6.31) after Maniar and Piccoli (1989) all the samples plot are in the orogenic field.

Table 6.4: Major element composition for the granite of the area (wt %)

Major Oxides	SP-01	SP-02	SP-03
SiO_2	58.92	64.24	59.21
TiO_2	00.93	01.51	00.84
Al_2O_3	15.64	13.57	16.32
Fe_2O_3	04.01	00.97	03.57
FeO	05.00	07.10	04.88
MnO	00.12	00.24	00.14
MgO	04.09	01.36	04.03
CaO	06.83	05.16	06.54
Na_2O	03.78	04.00	03.65
K_2O	00.42	01.27	00.63
P_2O_5	00.26	00.17	00.19
CIPW Norm			
Quartz	15.84	21.33	14.82
Orthoclase	02.25	07.24	03.90
Albite	31.96	33.56	30.92
Anorthite	24.46	15.58	26.13
Diopside	04.18	07.65	04.64
Hypersthene	13.46	08.70	13.46
Magnetite	05.80	01.39	05.10
Illmenite	01.82	02.74	01.67
Apatite	00.67	00.33	00.34
Niggli Values			
al	29.82	30.43	31.12
fm	33.72	30.89	33.26
c	23.78	21.05	22.76
alk	12.67	17.62	12.84
si	191.42	244.85	192.02
qz	40.74	74.37	40.66
k	03.16	01.35	01.83
mg	00.33	00.91	00.32
p	00.39	00.46	00.19
ti	02.34	04.12	02.14

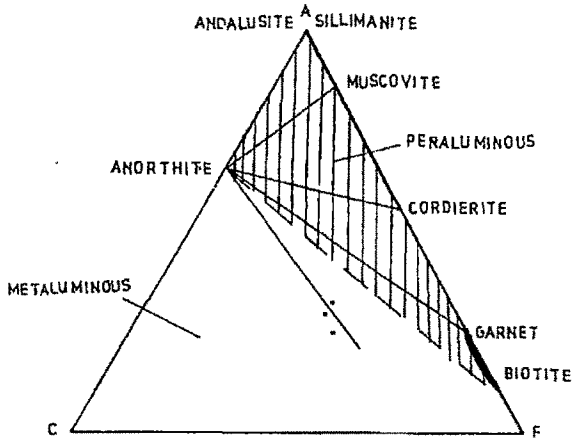

Fig.6.20 ACF triangular diagram (after Chappell and White, 1992) for the analyzed granite showing metaluminous chemistry.

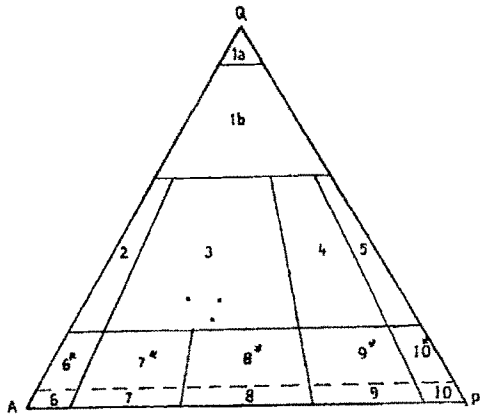

Fig.6.21 Normative QAP diagram for the analyzed granite. The fields are after Streckeisen (1976) 1a- quartzites ; 1b- quartz rich granitoids; 2- alkali feldspar granite; 3- granite; 4- granodiorite; 5- tonalite; 6*- quartz alkali feldspar syenite; 7- quartz syenite; 8*- quartz monzonite; 9*- quartz monzonite/ quartz monzo gabbro; 10*- quartz diorite/ quartz gabbro/ quartz anorthosite.

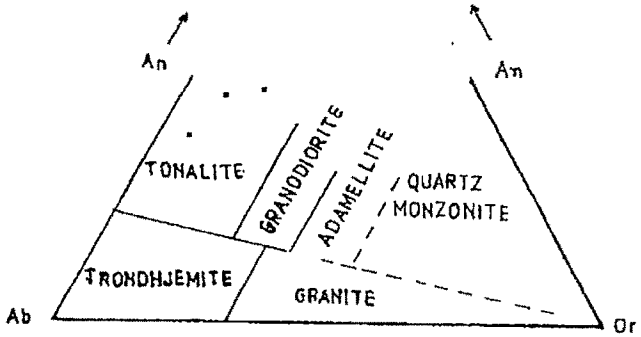

Fig.6.22 Plots of the analyzed granite on normative Ab- An- Or diagram (after O'Connor, 1965)

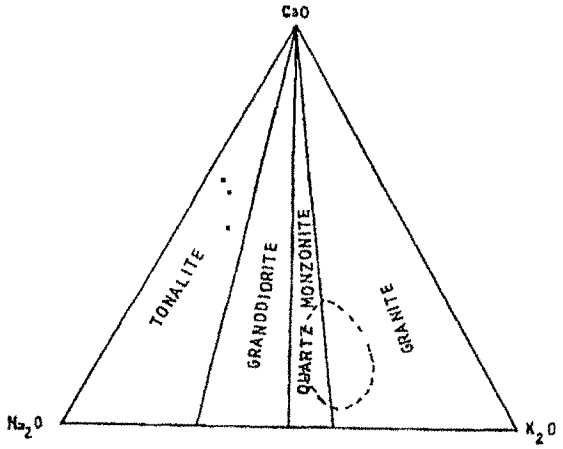

Fig.6.23 Plots of analyzed granite in Na_2O – CaO – K_2O triangular diagram (after Ali and Rao, 1980).

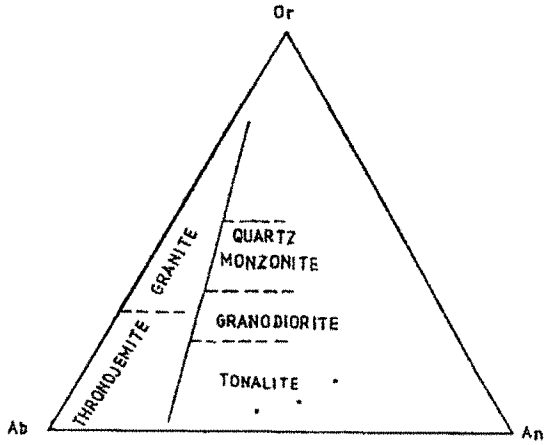

Fig.6.24 Normative Or – Ab – An triangular diagram (after Iden, 1981) for the analyzed granites.

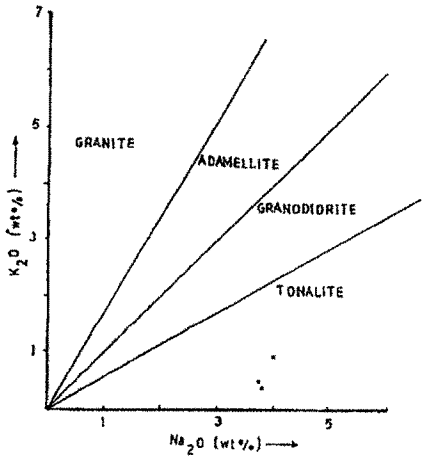

Fig.6.25 Binary Na_2O versus K_2O diagram (after Harpum, 1963) for the analyzed granite.

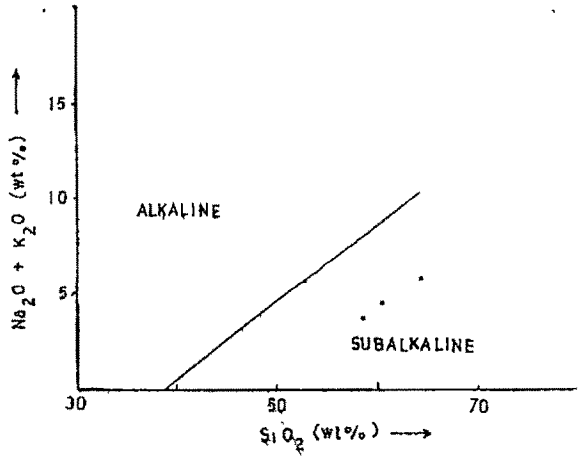

Fig.6.26 Plots of the SiO_2 versus $Na_2O + K_2O$ (after Irvine and Bavagar, 1971) of the analyzed granite.

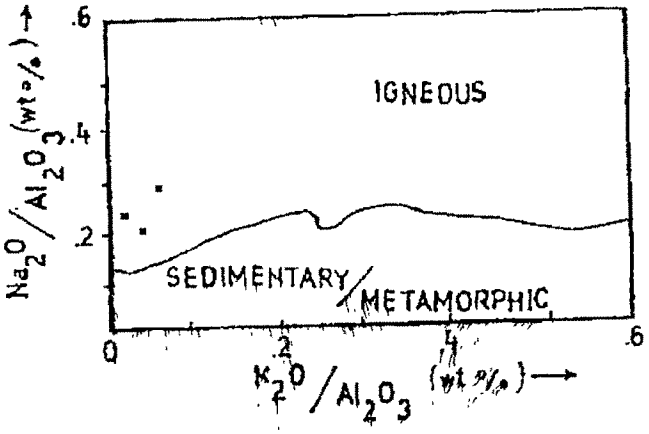

Fig.6.27 Plots of granites in K_2O/Al_2O_3 versus Na_2O/Al_2O_3 (after Garrels and Mckenzie, 1971) diagram.

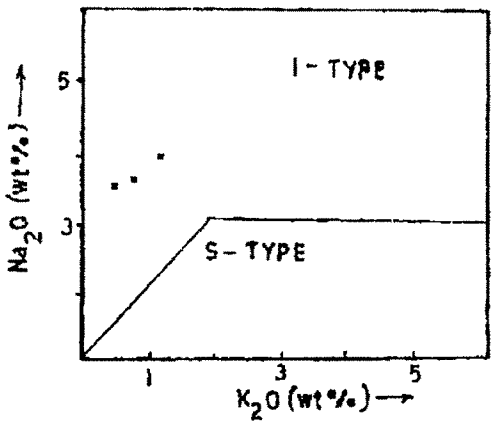

Fig.6.28 K_2O versus Na_2O diagram (after Chappell and White, 1992) for the analyzed granite.

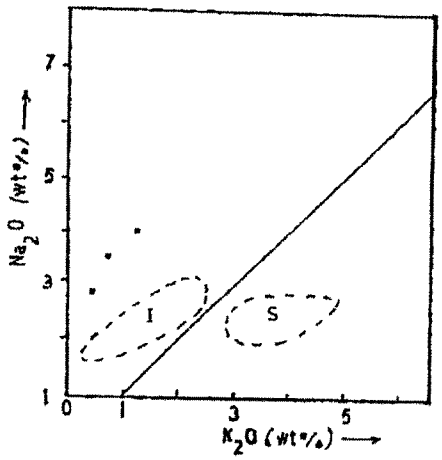

Fig.6.29 K_2O versus Na_2O plots (after Hine *et al*, 1978) for the analyzed granites.

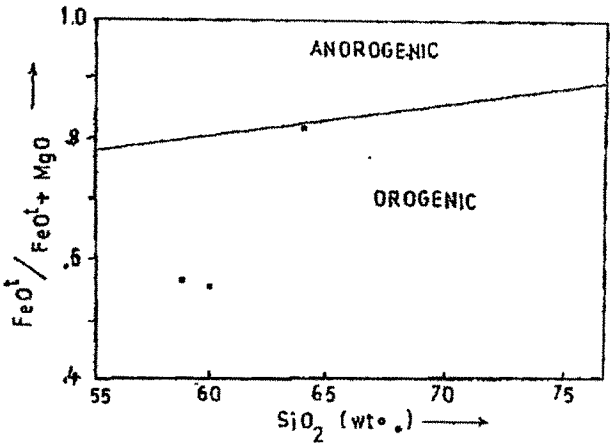

Fig.6.30 SiO_2 versus FeO/FeO + MgO plots (after Maniar and Piccoli, 1984) of the analyzed granites.

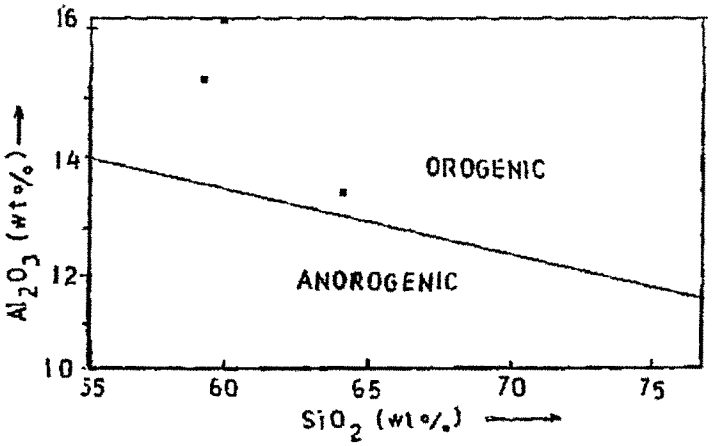

Fig.6.31 Plots of SiO_2 versus Al_2O_3 (after Maniar and Piccoli, 1984) of the analyzed granites.

6.3.6 Origin of the Granite

On the basis of field, petrological and petrochemical characters the origin of the granite is discussed as follows:

1. It occurs as dykes and veins in the quartzites.
2. It is massive and nonfoliated.
3. Contact is sharp with quartzites.
4. Characteristic texture is hypidiomorphic granular (Photo-6.5c).
5. Myrmekitic intergrowth between plagioclase and quartz is present (Photo-6.5d).
6. Perthitic intergrowth between potash feldspar and albite is present invariably (Photo-6.4c).
7. Rock is mainly composed of Potash feldspar, plagioclase, quartz and hypersthene.
8. Presence of euhedral grains of zircon (Photo-6.5b).
9. The granite is metaluminous as shown by the ACF triangular plot (Fig-6.20).
10. Plots in the QAP diagram indicate the granite falls in the field of granite (Fig-6.21).
11. The granite belongs to I-type as shown in the Na_2O/Al_2O_3 versus K_2O/Al_2O_3 plot (Fig-6.27) and Na_2O versus K_2O plot (Fig-6.28).
12. The granite samples fall in the field of orogenic granite as shown in the SiO_2 versus $FeO/FeO + MgO$ binary diagram (Fig-6.30) and SiO_2 versus Al_2O_3 diagram (Fig-6.31)

The granite of the study area is I-type granite having comparatively lower molecular ratio of $Al_2O_3/(Na_2O + K_2O + CaO)$, which suggests primary derivation of melt phase from the mantle, followed by subsequent assimilation of lower crustal rock. They are poor in quartz and high Fe_2O_3/FeO relative to S-type. This granite has varied mafic mineralogy and a variable amount of

pyroxene which is uncommon in normal granite. The granite seems to be intruded the country rock during waning phase of deformation of mobile belts, associated with extensional tectonics.